Amino acids as molecular linchpins in fundamental prebiotic processes

Udita Bandyopadhyay
IISER Pune https://orcid.org/0009-0001-7264-0934
Souradeep Das
IISER Pune https://orcid.org/0009-0008-1866-4119
Sahil Mulewar
IISER Pune
Tejashwini R
IISER Pune
Sudha Rajamani
srajamani@iiserpune.ac.in
IISER Pune https://orcid.org/0000-0002-6030-495X

Research Article

Keywords: Prebiotic heterogeneity, amino acid co-solutes, nonenzymatic replication, protocells, compartmentalization

Posted Date: October 16th, 2025

DOI: https://doi.org/10.21203/rs.3.rs-7866707/v1

Additional Declarations: The authors declare no competing interests.

Abstract

Amino acids are hypothesized to have been present on the early Earth via Urey-Miller type abiotic processes, in addition to being delivered via exogenous chondritic meteorites. Their potential coexistence in the primordial soup with RNA, amphiphiles and other co-solutes, highlights the importance of characterizing how they would have influenced various prebiotic processes. In previous studies, amino acids have been shown to interact with protocellular moieties and affect nucleotide oligomerization. Nonetheless, the outcome of such interactions on templated RNA replication, and on the physicochemical properties of single chain amphiphile-based protocells, is largely unknown. In this work, we characterize how amino acids affect RNA copying chemistry in their role as crucial prebiotic co-solutes. Additionally, we show how amino acids can promote self-assembly of fatty acid vesicles even under suboptimal pH conditions. Overall, our study shows that amino acids influence both information copying as well as compartmentalization, underscoring their importance in shaping the molecular pathways crucial to life's origin. In all, this study highlights how interactions between early biomolecular systems would have affected their subsequent co-evolution, which eventually would have set the stage for the transition of chemistry to biology on the early Earth.

1. Introduction

The prebiotic milieu is hypothesized to be a heterogenous mixture of several biomolecules that coexisted together, making it chemically diverse and potentially 'messy' (Monnard, 2016; Guttenberg et al., 2017; Vincent et al., 2021). Interactions between these foundational molecules is posited to have resulted in the formation of more complex building blocks and oligomers that eventually would have come together to result in protocells. Primordial cells are evolvable minimal entities with mainly three subsystems- a heritable polymer and a minimal metabolic network, encapsulated within a boundary system (Gánti, 2003). One major class of molecules that plays a prominent role in the aforementioned processes is amino acids, which also form the backbone of proteins that facilitate all metabolic processes in modern cells. Amino acids have been detected in interstellar ice and carbonaceous chondrites, which are thought to have been delivered via meteorites and interplanetary dust particles (IDPs) during bombardment of the Earth in the early Hadean period (Lawless and Yuen, 1979; McCollom et al., 1999; Simoneit et al., 2007). Additionally, they could have been readily synthesized via abiotic reactions in certain niches of the early Earth (Miller, 1953; Miller and Cleaves, 2006). All these evidences point conclusively towards the presence of amino acids on primordial Earth and their potential for interaction with other prebiotically relevant molecules in a myriad ways.

According to the RNA world hypothesis, RNA is considered one of the first informational polymers to have emerged on the early Earth (Gilbert, 1986). RNA also possess the ability to catalyze reactions, which would have eventually paved the way for the emergence of ribozymes (Carter, 2015; Cech, 1986). However, prior to this, RNA would have replicated via a nonenzymatic route in the compositionally heterogeneous prebiotic soup (Pate et al., 2015). Most of the studies involving nonenzymatic replication typically used a 'pure system' approach that allowed for the basic understanding of this phenomenon.

Nevertheless, these studies overlooked the inherent chemical complexity of the prebiotic soup, and how this would have affected crucial prebiotic reactions. Recently, more emphasis is on discerning how intermolecular interactions in a heterogenous soup could have affected the reaction outcomes of prebiotic processes. Given this heterogeneity, it is reasonable to assume that RNA (Joshi et al., 2022, 2021; Mayer et al., 2018; Rout et al., 2025; Sanchez and Renard, 2002) replication would have also occurred in the backdrop of a variety of molecules. These molecules, which are referred to as co-solutes, include, but are not limited to, amino acids, small organics, different salts, by-products of the other chemical reactions, etc. In this context, one of our previous studies showed how co-solutes like PEG and vesicles could have affected RNA replication (Bapat and Rajamani, 2015). This and other recent studies clearly demonstrate how the molecules present in the prebiotic chemical milieu, could have actively influenced the replication rate and its efficiency (Vogel et al., 2005; Patki and Rajamani, 2023; Rout et al., 2025). Extant cells contain a sophisticated machinery whose central player is an RNA polymerase enzyme which transcribes DNA to RNA. Notably, the catalytic power of this enzyme is governed by two Mg^{2+} co-factor ions and a few amino acids present in its active site (Carvalho et al., 2011). Nonetheless, it is not apparent how amino acid monomers or short acidic peptides corresponding to the active centre of the modern polymerase, could have affected nonenzymatic RNA replication. In this backdrop, we investigated how particular amino acids with different side chains would have affected nonenzymatic RNA replication (Fig. 1). Understanding this crucial prebiotic reaction could help in delineating how certain amino acids eventually came to be represented in the active core of enzymes.

Another process central to the emergence of life is the formation of protocell compartments, which would have been composed of amphiphiles that are hypothesized to have provided the requisite boundary condition, i.e. the membrane bilayer. The earliest bilayer-based membranes would have mainly comprised of single chain amphiphiles (SCAs), like fatty acids and their derivatives. These SCAs are postulated to be important prebiotic membrane forming components (Hargreaves and Deamer, 1978; Deamer W., 1985; Apel et al., 2002), crucial for protocell formation. These SCAs are ideal for primordial life due to their ability to form robust yet sensitive membranes that respond readily to environmental changes, and also for their ability to sequester molecules from the surrounding bulk environment without the requirement for any protein machinery (Mansy, 2010; Mansy and Szostak, 2009). Different kinds of lipidic SCAs like fatty acids, fatty alcohols etc, have been shown to be available due to delivery via exogenous meteorites and also by abiotic synthesis processes that may occurred on the early Earth (Lawless and Yuen, 1979; McCollom et al., 1999; Chyba and Sagan, 1992; Cohen et al., 2022). These fatty acid vesicles have been shown to get stabilized by certain amino acids, either by increasing their salt tolerance or by affecting their membrane lamellarity (Cornell et al., 2019). It has also been demonstrated that small dipeptides can bind with fatty acid membranes based on their charge and hydrophobicity (Xue et al., 2021). Given their ready availability in the prebiotic milieu, we set out to understand how amino acid monomers could have potentially also acted as a prebiotic bulk medium for fatty acid-based systems. Fatty acid vesicles are known to result only in a very stringent pH regime that is close to the apparent pK_a of the headgroup of the membrane forming amphiphile. In this study, we demonstrate that amino acids can act as a buffer and facilitate the assembly of vesicles at a pH that is away from the

system's optimum pH value. Relevantly, amino acids buffer several reactions in extant biochemistry and also feature prominently as a biologically pertinent Good's buffer (Borsook and MacFadyen, 1930; Good et al., 1966; Pielak, 2021). Further, we also demonstrate how interactions with amino acids can change the physicochemical properties of fatty acid membranes, driving their chemical evolution towards a possibly more robust membrane system (Fig. 1).

In all, this study explores the role of amino acids in two fundamental prebiotic processes that are postulated to have set the stage for the emergence of first cellular life. By bridging these two areas, i.e. nonenzymatic information transfer and compartmentalization, we show how amino acids could have played a vital role in shaping molecular evolution and early biochemical pathways that potentially led to the origin and early evolution of life (Fig. 1).

2. Materials and methods

Nucleoside-5'-phosphorimidazolides (ImpNs) were purchased from GlSynthesis Inc. The Cy3-tagged amino-G primer (3'-amino-2',3'-dideoxynucleotide) were purchased from Keck's laboratory (Yale, USA) and were gel purified before using. The RNA templates are purchased from Sigma-Aldrich (Bangalore, India) and were used without further purification. The amino acids are purchased from Sigma-Aldrich, and all are of analytical grade. For all the experiments and buffer preparation, filtered Nanopure water (18 MΩ) was used as the solvent.

Oleic acid/OA (cis-9, $C_{18}H_{34}O_2$) and all the amino acids i.e., glycine ($C_2H_5NO_2$), valine ($C_5H_{11}NO_2$), alanine ($C_3H_7NO_2$), serine ($C_3H_7NO_3$) and histidine ($C_6H_9N_3O_2$) were all procured from Sigma-Aldrich and were used without further purification. Bicine (N,N-Bis(2-hydroxyethyl) glycine) and CHES (N-cyclohexyl-2-aminoethanesulfonic acid) for buffers, and laurdan, pyrene and nile red dyes, were also purchased from Sigma-Aldrich.

2.1. RNA replication reaction set-up and collection of the time points

The reactions were set up at 25°C (room temperature, RT) in the thermomixer. At first, 1.3 μM of the particular template and 0.325 μM of the ddG-NH_2 primer were mixed and heated at 95^0 C for 5 mins, followed by cooling for 2 mins to bring it to the room temperature, and then spun down. 100 mM of Tris (pH 7) and 10 mM of $MgCl_2$ were added to this solution. The amino acid stocks were made in filtered nanopure water and the pH was adjusted to 7. Followed that, 10 mM of each amino acid was added to the reaction using appropriate volumes from the stock solution. The subsequent addition of the ImpN initiated the reaction. 1μL from these reaction mixtures was taken out during different time intervals as specific timepoints. The timepoints were stored in 7μL loading buffer (TBE) containing 8M urea and immediately stored in -40^0 C. It is to be noted that the duration of the reactions, and the corresponding collection of the timepoints for every reaction-set, were adjusted after initial standardization. The ImpN

stocks were freshly made before the start of the reactions, and the 0th timepoint was collected right after the addition of the ImpN, flash frozen and stored right away.

2.2. Gel quantification and analysis

The amino-primer is attached to a 5’ -Cy3 tag for its ready detection on urea gel. Before loading on to the denaturing gel, an unlabelled RNA primer having the same sequence as the amino primer (which was named ‘excess primer’), was added to each sample in 20 times excess concentration. When heated at 95^0 C for 5 mins, the labelled primers (extended or unextended) present in the reaction mixtures get separated from the template partners, allowing the ‘excess primer’ to now sequester the templates as they make for an able competitor RNA. A loading dye mix composed of bromophenol blue and xylene cyanol was also added to each sample for the easy tracking of the bands that get separated on the denaturing PAGE gel. All the timepoints are run on 20% denaturing gel having 8 M urea, in which the upper band represents the (N + 1) extended primer that results from templated replication, while the lower band represents the starting /unextended primer (N). The gels were scanned using Amersham Typhoon Imager (software version 2.0.0.6) at a 550V PMT and at a pixel size of 100 µm. Subsequent analysis was performed using ImageQuant TL (1D v8.2.0) software. For quantification of the bands, we calculated the fraction of N + 1 band using the following formula for the different timepoints.

$$\textit{Fraction N + 1} = \frac{Intensity\ of\ N{+}1\ band}{Intensity\ of\ (N\ band{+}(N{+}1)\ band)}$$

Fraction N + 1 that resulted over the course of the reaction (min), was plotted to get an idea of the overall trend of the reaction. The rates of the reactions were then calculated from the slope of the linear regression curve, by considering few early data points under the linear regime (Rajamani et al., 2010).

2.3. Vesicle Suspension Preparation

Vesicle suspensions were made using the thin-film rehydration method. The lipid film was made by drawing an appropriate amount of lipid solution from a 10 mg/ml stock of oleic acid in methanol. The methanol solvent was evaporated completely in a vacuum desiccator for 3 hours to prepare a dry thin-film of lipids. The obtained lipid film was then rehydrated with an appropriate volume of buffer or amino acid solution of intended pH (detailed in supplementary section S1), to make the required concentration of oleic acid vesicle suspension (see supplementary section S2). Important to note, in case of all amino acid solutions, only amino acid monomer of required amount were solubilized in nanopure water and pH was adjusted with required amount of Sodium hydroxide (NaOH). No Good’s buffer was added while preparing the the amino acid solutions. The suspension was then vortexed vigorously to make the it homogeneous, and then kept overnight for equilibration in an Eppendorf Thermomixer C (Hamburg, Germany) at RT.

2.4. Microscopy Analysis

3 mM oleic acid suspensions were prepared using the thin-film rehydration method. Suspensions were prepared with the respective amino acid solutions in CHES buffer (control) at pH 9.6. These samples

were visualized using Differential Interference Contrast (DIC) microscopy and epifluorescence microscopy using a Carl Zeiss Axio Imager A1 Apotome microscope and a Leica DM6 upright microscope, at 40X magnification (NA = 0.75). 8μL of the sample was placed on the glass slide and covered using a glass coverslip. The coverslip was sealed and the samples were imaged soon thereafter. For Epifluorescence microscopy, samples were stained with 3μM Nile red dye after vesicle suspensions were made. These samples were imaged using a DsRed filter. Acquired images were further processed using Fiji ImageJ software package.

2.5. Solvatochromic probe assays

a. 3μM pyrene was added in each vesicle suspension, and this was incubated for at least 15 minutes at RT before subjecting it to fluorescence spectroscopy. Each sample was excited at 335 nm, and the emission spectra were obtained between 350 and 600 nm. The maximum intensity of the broad excimer peak was observed around 470 nm (I_{ex}). The excimer intensity I_{ex} was normalised with intensity at 372 nm (I_1), yielding I_{ex}/I_1. I_{ex}/I_1 is inversely proportional to the vesicle content in the suspension.
b. 3μM laurdan was added to each vesicle sample and resuspended in a similar manner as mentioned above. Redshift of laurdan was calculated by the parameter generalized polarization (GP), which is defined as, $GP = (I_{450}-I_{510})/(I_{450} + I_{510})$. Here, I_{450} is the corresponding intensity at 450 nm wavelength which is the peak for the ordered phase of the membrane and I_{510} is the intensity at 510 nm. i.e., the peak for the disordered phase. Each sample was excited at 350 nm, and the emission spectrum and anisotropy were both recorded. For all these fluorescence measurements, Fluoromax-4 (Horiba Ltd., Kyoto, Japan) was used. All the data were plotted using Graphpad Prism 10 (Supplementary section S2).

2.6. Dynamic light scattering (DLS)

All the lipid suspensions were subjected to DLS using a 633 nm fixed laser in the Malvern Panalytical Zetasizer Nano ZS90 (Malvern, UK), and the data was recorded at 25°C while using a 90° right angle scatter detector. For each sample, the side scattering was measured for obtaining size-intensity distributions and the mean diameter. The size-intensity distribution data was then plotted as a Gaussian distribution wherein the total area under the curve for each plot amounts to 100% (Figure S4, Supplementary section S3). The mean size was plotted (marked by line in the box) as a box plot with the maximum and minimum range of values obtained over three independent experimental replicates. All of this data was plotted using Graphpad Prism 10.

3. Results

3.1 Effect of amino acids on nonenzymatic templated-replication of RNA in the presence of Mg^{2+}.

Nonenzymatic template-directed replication has been studied by systematically characterizing primer extension using activated or non-activated nucleoside monophosphates (Orgel, 2004; Bapat and

Rajamani, 2015; Walton et al., 2019; Dagar et al., 2022). In these reactions, the template is paired with an RNA primer, where the primer gets extended by the addition of an incoming nucleotide (Walton et al., 2019). For this study, phosphorimidazolide monomers (ImpN) have been used as activated incoming nucleotides against their cognate template bases. This leaving group (imidazole) modification of the nucleotide is essential for the primer extension in the absence of an enzyme or catalyst (Duzdevich et al., 2021). In addition to the contributions from the stereochemistry of the extending terminus and the chemistry of the incoming nucleotide, metal ions play a very important role in the replication process by stabilizing the RNA backbone and masking the negative charges so that the primer and the template can form a stable duplex.(Szostak, 2012).

Previous studies from our lab and other groups were mostly done in the presence of 200 mM NaCl as the main counterion in the reaction mixture (Rajamani et al., 2010; Patki and Rajamani, 2023). However, for this study we adapted the system for Mg^{2+}, considering the presence of this metal ion as a cofactor in several modern enzymes including the ones involved in replication (Carvalho et al., 2011). In this backdrop, we studied how individual amino acid monomers, when added in equal concentration to that of Mg^{2+} ions, would affect the reaction rates. Specifically, we aimed to understand how the charged groups of amino acid side chains would affect templated-replication rates. Six different amino acids were evaluated as co-solutes in the aforesaid nonenzymatic templated RNA replication paradigm. Aspartic acid and glutamic acid were chosen as the negatively charged candidates, while arginine and lysine were chosen as the positively charged candidates. Histidine and glycine were chosen as representatives for neutrally charged candidates (Supplementary Table 1). The working concentration of Mg^{2+} used (10–20 mM), is similar to what has been used in previous origin of life studies (Adamala and Szostak, 2013; Szostak, 2012). The nonenzymatic replication control reactions were compared with the ones that were carried out in the presence of amino acids. Each reaction was assigned a reaction name and this has been mentioned in Supplementary Table 1 along with the details of the primer and template sequences used.

The control reaction rates were first measured for the addition of ImpG across templating base C (represented as G_C) (Fig. 2). The average rate for this control reaction was 1.01 $hour^{-1}$ (N = 3). The subpanels A (of panels 1–4) in the Fig. 2 shows representative images for the denaturing gels that were acquired (quadrants 1–4, each gel image corresponds to a specific reaction), and these were used to quantify the intensity of the fluorescently labelled bands obtained for the various time points (see Method section 2.2). The overall reaction kinetics for a given reaction is shown in the subpanels B of panels 1–4 in Fig. 2. To measure the individual pseudo-first order reaction rates, the initial rates of the reactions were acquired by fitting the first several data points for both the control and test reactions that were carried out in the presence of amino acids. Subpanels C for 2, 3 and 4 panels, depict the rates obtained for reactions that were carried out in the presence of histidine, aspartic acid and lysine, respectively. The rates for G_C reactions with His, Asp and Lys were reduced to 0.36 $hour^{-1}$, 0.31 $hour^{-1}$, and 0.70 $hour^{-1}$, respectively (rounded off to two decimal places, N = 3), a clear reduction from the control experiment rate (1.01 $hour^{-1}$).

The effect of amino acids was evaluated for all the four different Watson-Crick base pairing reactions detailed in Supplementary Table 1i.e. addition of ImpG across templating base C, addition of ImpA across templating base U, addition of ImpC across templating base G and the addition of ImpU across templating base A. Differences in the reaction rates were seen in all the test reactions when compared to the corresponding control reactions. Pertinently, the rates for the control reactions performed only in presence of Mg^{2+}, were very different across the four Watson-Crick base paring templated reactions (Figure S1). The average rates were obtained from three reaction replicates for all the six amino acid variations that were performed for each primer-template combination, as detailed in Supplementary Table T2. In addition to these reactions, to examine whether Mg^{2+} showed any additive effect when present with Na^{+}, a parallel set of experiments was performed where 200 mM Na^{+} was added along with 10 mM Mg^{2+} in the four control reactions (without amino acids). Notably, the rates for these reactions did not significantly change when compared to the only Mg^{2+}control reactions (Figure S2). The effect coming from 10 mM and 20 mM histidine (Figure S3), was evaluated in the presence of 200 mM NaCl as this was the amino acid that affected the extension rates the most. However, the rate obtained was not significantly different from what was seen when Na^{+} alone was used as the counter ion in the reaction (Figure S3). All these variations clearly indicated that Mg^{2+} remained a dominant influence in the replication processes studied.

Statistical analysis was performed to check how the test reactions compared to the corresponding control reactions. Figure 3 shows the comparative effects obtained for the six different amino acids when present along with 10 mM Mg^{2+}, across all the different primer-template complexes studied. Notably, the six amino acids used in this study affected the four primer-template complexes differently. Upon the addition of amino acid to the reaction mix, the rates dropped significantly for some amino acids in case of A_U, G_C and C_G reactions. In case of A_U reactions all six amino acids resulted in a significant reduction in the reaction rate (Fig. 3A). In case of C_G reactions, His, Gly, Asp and Glu resulted in a significant reduction in rates, while in G_C reactions, His and Asp showed the most significant effect. Notably, in case of U_A reactions, the effects were the least prominent for all the six amino acids. It is relevant to point out that for a meaningful comparison, we kept the concentration of the co-solutes (amino acids) same across all the reactions (10 mM) and equimolar to the metal ion used. We used 10 mM amino acid even in the U_A reactions despite the relatively higher concentration of ImpU used in the control reaction. ImpU is often used at 40 mM concentration because U incorporates less efficiently and hence at a slower rate across its templating base A (Patki and Rajamani, 2023).

Based on our results, it is apparent that His and Asp are the amino acids that reduce the reaction rates the most (as detailed above), especially in the faster reactions like A_U and C_G where the effects are prominent. While previous studies have demonstrated how certain co-solutes affect the fidelity and accuracy of nonenzymatic RNA replication (Bapat and Rajamani, 2015; Patki and Rajamani, 2023), this study adds a new dimension to our understanding of nonenzymatic reaction dynamics from the perspective of amino acids and divalent metal ions, two crucial prebiotic co-solutes. There are several possibilities for why this rate reduction could be happening in the presence of amino acids. (1) The

presence of certain amino acid residues could be sterically hindering or electrostatically interfering with the optimal alignment of the reactive groups that facilitate primer extension. These interactions can potentially perturb the active site geometry or alter local charge distribution. (2) The crowding effect, as discussed in the introduction section and also mentioned in recent studies (Bapat and Rajamani, 2015), stems from the presence of co-solutes in the surrounding vicinity that affect the reaction rates. (3) When the activated nucleotide is present in the same concentration as the amino acid (along with Mg^{2+}) in the reaction medium, there is the possibility of formation of an NMP-amino acid adduct as a reaction intermediate (Namani and Walde, 2005; Roy et al., 2024). This may act as a competitive inhibitor for the incoming cognate monomer, thereby resulting in a decrease in the reaction rate.

3.2.1 Amino acids act as a bulk medium supporting prebiotic vesicle formation at suboptimal pH.

Another important role that amino acids might have played in a complex prebiotic milieu is facilitating the compartmentalization of protocells. The pH-dependent self-assembly of prebiotic membranes is hypothesized to have been dominated by single-chain fatty acids (Sarkar et al., 2020). For protocell formation under lab conditions, the pH of the bulk solution is typically maintained using Good's buffers like Tris, CHES, bicine, etc. However, the pH of a prebiotic soup was potentially not regulated by such buffers. Since prebiotically plausible SCA membranes are very sensitive to pH fluctuations, their stability when the pH deviates away from the apparent pK_a of the fatty acid has been a problem while fabricating protocells. Previous studies have investigated the interactions between membranes and amino acid monomers/small peptides, and suggested that both electrostatic interactions and hydrogen bonding are relevant modes of crosstalk (Cohen et al., 2024; Cornell et al., 2019; Xue et al., 2021). Some studies have also shown that amino acid interactions increase the robustness of prebiotic membranes against higher salt concentrations (Cornell et al., 2019).

In this backdrop, we investigated whether amino acids could assist SCA-based vesicle self-assembly away from its apparent pK_a, by acting as a plausible prebiotic buffering agent. To do this, we exploited the basicity of the primary amine group of the amino acids to see if it could provide a buffering medium at pH 9.6 to facilitate vesicle formation. We show that amino acids do indeed play the role of a buffering medium, while also acting as co-solutes that interact with membranes, as has been shown in past studies (Cornell et al., 2019; Xue et al., 2021). Notably, the conditions used in this regard simulate prebiotically relevant conditions like what could have been possible in a heterogeneous prebiotic niche. It also further highlights the multiple roles that amino acids would have played in important prebiotic processes, underscoring a concerted evolution of different biomolecules on the early Earth. In this study, oleic acid (OA), a monounsaturated 18-carbon (C18) fatty acid, was used as the model membrane-forming amphiphile, while glycine, valine, alanine, serine and histidine were chosen for the amino acids.

Glycine, valine and alanine are among the primordial amino acids that are also thought to be the most abundant on the prebiotic Earth (Ikehara, 2014, 2005; Koga and Naraoka, 2017). Since we also wanted to

understand the role of amino acid side chains and how their polarity could have impinged on interactions with membranes, serine, also a prebiotically relevant amino acid, was used because of the hydroxyl group in its side chain (Koga and Naraoka, 2017). As for histidine, it was selected even though it is not considered as prebiotically relevant, in order to characterize amino acids with an aromatic side chain. All these amino acids have a backbone amino group pK_a in the range 9-9.7, which makes them good candidates for use as prebiotic buffers in this study (Supplementary Table T3). It is to be noted that at the pH used in this study (i.e. 9.6), while valine and alanine with their isopropyl and ethyl side chains, respectively, are slightly hydrophobic. Serine, which has a primary alcohol in its side chain, has the potential to participate in hydrogen bonding, while histidine has an aromatic imidazole group in the side chain.

Oleic acid is known to have an apparent pK_a of ~ 8.5, and has been shown to self-assemble into membranes in the pH range of 8–9 (Monnard and Deamer, 2003). This pH-specific membrane formation is due to hydrogen (H) bonding between the protonated and deprotonated head groups of oleic acid (50% of each), which results in a pseudo-diacyl like structure that assists bilayer formation (Sarkar et al., 2020). In this study, we have used bicine buffer of 200 mM (pH 8.5) as the positive control as it is the optimum condition for the self-assembly of oleic acid vesicles. However, at pH 9.6, membrane formation was not observed, as expected, when using a synthetic goods buffer like CHES (200 mM, used as a negative control), as this pH deviates from the optimum pH for C18 vesicle formation (Fig. 4). At pH 9.6, the Henderson-Hasselbalch equation suggests that 92.6% of oleic acid monomers should be deprotonated (hydrogen bond acceptor), while 7.4% should be in the protonated state (hydrogen bond donor). This is, however, not suitable for membrane formation via pseudo-diacyl structure formation. Notably, when added to an amino acid solution at pH 9.6, which is equimolar to the control CHES buffer (200 mM), the addition of oleic acid (5 mM) did not change the pH of the solution, as it is a weak acid, confirming the amino acid solutions' buffering ability.

In all the amino acid solutions studied (at pH 9.6), vesicle formation by oleic acid was observed even at this suboptimal pH, while no vesicles were seen when a pH 9.5 synthetic goods buffer of 200 mM CHES was used. Notably, the effective critical vesicle concentration (CVC) of the oleic acid system was not significantly affected due to the amino acid bulk solution. This observation is consistent with another study that showed that interaction with amino acids and dipeptides does not change the system's CVC (Xue et al., 2021). These observations suggested that the amino acids might be compensating for the smaller number of oleyl hydrogen bond donors present at pH 9.6, thereby facilitating membrane formation. Previous studies have shown that amino groups can act as both hydrogen bond donors as well as acceptor, as they form hydrogen bonds with water molecules (Ishigami et al., 2015; Romero Nieto et al., 2017). We hypothesize that in our study, the amino group in the backbone is possibly acting as a hydrogen bond donor, which facilitates membrane assembly at pH 9.6. (which is ~ 1 pH unit greater than the apparent pKa of oleic acid membranes).

Further, the size distribution of the resultant vesicles formed in bulk solutions of amino acids, were characterized using dynamic light scattering (DLS) and compared to the optimum size distribution that

was obtained at pH 8.5. The DLS data showed the mean sizes of the vesicles (diameter, d) at their optimum pH of 8.5, as being significantly higher than the vesicles that were formed using amino acid buffers at pH 9.6 (Fig. 5a). At pH 8.5, the mean size was around 400 nm (marked by the red line in Fig. 5a), whereas the ones that resulted in the amino acid buffers were predominantly in the size range of 100–200 nm. The vesicles that resulted in glycine and valine amino acid buffers, showed significantly lower mean diameter of 115 and 121 nm, respectively. All the other amino acid buffers resulted in vesicles with a diameter range of 150 nm to 200 nm.

Since glycine has no prominent side chain while valine contains a sizeable hydrophobic side chain, the aforementioned decrease in the vesicle size may not necessarily be only from the hydrophobic nature of the amino acid. This corroborates a previous study that showed no strong correlation of hydrophobicity with the binding of peptides to decanoic acid membranes (Xue et al., 2021). However, the overall decrease in the mean vesicle size across all amino acid buffers might have resulted due to a difference in bilayer content per vesicle, occurring under these conditions. Nonetheless, these results confirm the formation of vesicles in the presence of amino acids, even when the pH was suboptimal. Pertinently, all the five amino acids used in this study facilitated vesicle formation despite bearing chemically different side chains. Importantly, the smaller size of the resultant vesicles hinted at a possible change in the physical or chemical properties of the membrane in the presence of amino acid buffers (at pH 9.6). In all, these observations highlighted how the role of complexity in the prebiotic milieu, e.g. coexistence of amino acids and fatty acids, could have affected each other's properties, as is seen in the increased propensity for vesicle formation in this case.

3.2.2 Impact of different amino acids in regulating physicochemical properties of prebiotic membranes.

The next question was to ask if this membrane-amino acid interaction was somehow impacting the physicochemical property of the (resultant) membrane. To probe this, different solvatochromic fluorescent probes were used. Pyrene was used to estimate total bilayer content in each lipid suspension across the five amino acids (Fig. 5b). Excimers of pyrene molecules that form in the bilayer structure are measured using a ratiometric calculation of I_{ex}/I_1, where I_{ex} is the maximum intensity of the pyrene excimer peak and I_1 is the maximum intensity of the first vibronic peak of the pyrene spectra (Sarkar et al., 2021) (Methods section 2.5). The I_{ex}/I_1 ratio of pyrene is inversely proportional to the total bilayer content present and the bilayer content in amino acid buffers (at pH 9.6) was compared to optimum bilayer forming conditions for oleic acid vesicles, i.e. pH 8.5.

It was observed that in all other amino acid buffers excepting for valine, the total bilayer content was significantly higher than when the vesicles were formed at the optimum pH of 8.5 (Fig. 5b). Another important observation was that valine, being the most hydrophobic amino acid among the five amino acids studied, resulted in bilayer content that was very similar to what is observed at the optimum condition of pH 8.5. In the case of other amino acids, the membrane property, in terms of total bilayer content, did show an increase upon interaction with amino acids. Further, the ratio of the first (I_1) and

third (I_3) vibronic peaks of pyrene (I_1/I_3 ratio), which indicates the micropolarity of the bilayer (Sarkar et al., 2021), typically decreases upon a decrease in the micropolarity of the membrane. Upon vesicle formation at pH 9.6, we observed that this I_1/I_3 was lower for the vesicles that resulted in the presence of amino acids when compared to the vesicles that were obtained at the optimum pH of 8.5 in bicine buffer (Figure S5).

Laurdan generalized polarization (GP) value is another important parameter that tells us about the lipid order of the membrane indicating whether is it ordered or disordered (Method section 2.5). A more positive GP value suggests less water activity in the membrane and, in turn, higher order. The GP values of the vesicles that resulted in the presence of the amino acid buffers were more positive when compared to the GP value of the vesicles formed in pH 8.5 buffer, across all the amino acids tested (Fig. 5d). This indicated that the vesicles that formed in the presence of amino acids had less water activity in the bilayer and more order when compared to the vesicles that formed in the absence of amino acids (in bicine buffer, pH 8.5). This change in physicochemical property of the membrane suggested that the amino acid interaction with the membrane was causing water exclusion from the membrane, making this prebiotically relevant membrane a more robust and stable structure. Among all the amino acids tested, the decrease in micropolarity was most significant for histidine. In both pyrene and laurdan GP assays, the deviation of physicochemical properties of the resultant membranes were highest in the presence of histidine. This observation could be attributed to the imidazole ring of histidine, which has been shown to interact near the headgroup of the amphiphile via hydrophobic interactions with the membrane, thereby resulting in an increase in the GP value of the bilayer (Suga et al., 2017).

Further, the membrane anisotropy was also measured using laurdan to probe the membrane fluidity of the vesicles (Fig. 5c, lower anisotropy means more fluid membranes). Anisotropy was significantly lower for vesicles in histidine buffer than in any other amino acid sample. This suggested that the membranes formed in the presence of histidine were significantly more fluid, also suggesting that the aromatic imidazole side chain of histidine is probably able to penetrate the bilayer of the lipid amphiphile in a way that results in an increase in the membrane fluidity. This hydrophobic interaction decreases the access of water into the bilayer (Suga et al. 2017, Fig. 5c & 5d), indicating a decoupling of the membrane bilayer property between the head group region and the acyl tail core region in the presence of the histidine monomers (Suga et al., 2017; Tauchi et al., 2018). This is somewhat analogous to how cholesterol impacts a cell membrane (Mishra and Chakraborty, 2023), with a more primitive comparison being with that of isoprenoid groups that have been shown to impart a similar property of increasing fluidity in archaeal membranes (Albers and Meyer, 2011). Relevantly, all other amino acid effects showed insignificant deviation from the optimum that was observed in the control vesicles made at pH 8.5.

The above results, along with previously published data, suggest that amino acids can change the microproperties of membranous vesicles depending on the nature of their side chain. Vesicle content seemed to be highest in the presence of alanine and histidine followed by serine, and then followed by glycine and valine (Fig. 5b). The solvatochromic probe studies do not indicate any clear trend attributable

to hydrophobic-hydrophilic interactions with the side chain of the amino acids used. Nonetheless, it strongly suggests that there are more forces at play between the amino acids and the interacting membranes. Specifically, the laurdan studies suggest that the aromatic imidazole side chain of histidine was able to maximally impact the physicochemical properties of these membranes.

4. Discussion

In this work, the dual role of an important biomolecule, i.e., amino acids, has been systematically characterized in the context of two relevant prebiotic processes. Our results show that it acts as a co-solute impinging on prebiotic information transfer reactions, while also providing an interesting bulk medium that increased prebiotic self-assembly. In the context of nonenzymatic replication, the amino acids with charged sidechains were the most antagonistic. Conversely, these amino acids also enhanced the stability of SCA vesicles when employed as a buffering medium. Among all the amino acids studied, histidine and aspartic acid showed the most pronounced effect on nonenzymatic RNA replication reactions. However, when present alongside a metal cofactor like Mg^{2+}, they improved the replication rate, possibly because of being coordinated in a better orientation in this scenario.

Previous studies on amino acid-nucleotide interactions show that they are multifaceted, involving both backbone and side-chain contributions. Positively charged and polar amino acids are most frequently involved here, with specific preferences for certain nucleotide bases (Jeong et al., 2003; Hoffman et al., 2004). Relevantly, co-solutes or co-solute proxies in the prebiotic soup have been shown to significantly alter the kinetics and fidelity of nonenzymatic RNA replication (Bapat and Rajamani, 2015; Patki and Rajamani, 2023). Building upon these insights, our study elucidates the role of amino acids as a potent co-solute that can also modulate nonenzymatic templated replication of RNA, by engaging in specific chemical interactions thereby affecting the copying chemistry. Thus, by bridging the gap between molecular crowding and direct chemical modulation, this work reveals how amino acids could have also influenced early RNA replication.

As for SCA vesicles, they are a good model candidate for protocell compartments. However, they do pose a problem due to their inherent instability. Fatty acids by themselves cannot sustain stable membrane vesicles under substantial fluctuations of external conditions in the environment like pH, temperature, high salt concentrations, etc (Maurer, 2017). Our results involving amino acids assisting vesicle formation even at suboptimal pH highlight the importance of how the interplay between different building blocks of life in a putative primordial soup could have mitigated otherwise unfavourable outcomes. And, our results strongly indicate that amino acids interaction with fatty acid membranes seems to depend on their side chain. Previous studies have suggested that intermolecular hydrogen bonding does play a prominent role in membrane-amino acid interactions (Cornell et al., 2019; Xue et al., 2021). This hydrogen bonding between the different amino acids and oleic acid membranes could be the stabilizing force that facilitates vesicle formation at a pH regime higher than the optimum. All the amino acid buffers examined in our studies deviated from the optimum buffered condition of pH 8.5, showing significant changes in membrane order and total bilayer content. Our study provides evidence that amino

acids indeed have a significant impact on the membrane's microproperties, including water accessibility, fluidity and micropolarity; compared to what was observed in vesicles that resulted from an otherwise optimum buffered condition of pH 8.5. Notably, our results highlight that this amino acid-membrane interaction, results in the most prominent alteration of membrane properties in the case of histidine that has an aromatic side chain. Simultaneously, the interaction with histidine also seemed to make the membrane more dynamic, indicating that such co-solute interactions of SCA membranes with amino acids, could have been more conducive for shaping early protocell evolution.

Dehydration-rehydration (DH-RH) cycles in terrestrial geothermal pools would have been readily facilitated by relevant geological phenomena (Damer and Deamer, 2020). During DH-RH cycles, molecules like amino acids can reach transiently high concentrations (Deamer, 2015), leading to the possibility that amino acids could have acted as prebiotic buffers, facilitating the formation of robust vesicle systems. This is not surprising given how amino acids play an important role in buffering various reactions, even in extant biology (Borsook and MacFadyen, 1930; Good et al., 1966; Pielak, 2021). Moreover, a recent study from our group shows that amino acids could have facilitated the formation of longer nucleotide oligomers (and in greater yields) under prebiotic conditions (Roy et al., 2024). Taken together, one can envisage how such interactions in a chemically heterogeneous prebiotic soup, which comprised a mixture of amino acids along with other pertinent biomolecules such as RNA oligonucleotides, lipidic amphiphiles, and other interacting chemical moieties, could have shaped early biomolecular evolution. Pertinently, amino acids could have played an important role as the building block that connected all the nonenzymatic prebiotic processes in these niches. However, further studies involving increasingly complex prebiotic mixtures are required to help shed light on why life especially evolved with amino acid-based proteins as the linchpin of many fundamental biochemical processes that are known today.

Declarations

Acknowledgements

The authors wish to extend their special thanks to the Microscopy Facility at IISER Pune. Also, the authors would like to thank COoL lab members for their feedback on the work.

Funding statement

SR acknowledges research support from IISER Pune, Department of Science and Technology's Science and Engineering Research Board (SERB, Grant No. CRG/2021/001851) and Department of Biotechnology, Govt. of India (Grant No. BT/PR43193/BRB/10/2006/2021). UB and SD wish to thank UGC and CSIR, Government of India for fellowship support.

References

1. Adamala K and Szostak JW. Non-Enzymatic Template-Directed RNA Synthesis inside Model Protocells. Science 2013;342(6162):1098–1100; doi: 10.1126/science.1241888.
2. Albers SV and Meyer BH. The Archaeal Cell Envelope. Nat Rev Microbiol 2011;9(6):414–426; doi: 10.1038/nrmicro2576.
3. Apel CL, Deamer DW and Mautner MN. Self-Assembled Vesicles of Monocarboxylic Acids and Alcohols: Conditions for Stability and for the Encapsulation of Biopolymers. Biochim Biophys Acta - Biomembr 2002;1559(1):1–9; doi: 10.1016/S0005-2736(01)00400-X.
4. Bapat NV and Rajamani S. Effect of Co-Solutes on Template-Directed Nonenzymatic Replication of Nucleic Acids. J Mol Evol 2015;81(3–4):72–80; doi: 10.1007/s00239-015-9700-1.
5. Borsook H and MacFadyen DA. THE EFFECT OF ISOELECTRIC AMINO ACIDS ON THE pH+ OF A PHOSPHATE BUFFER SOLUTION : A CONTRIBITTION IN SUPPORT OF THE “ZWITTER ION” HYPOTHESIS. J Gen Physiol 1930;13(5):509–527; doi: 10.1085/jgp.13.5.509.
6. Carter CW. What RNA World? Why a Peptide/RNA Partnership Merits Renewed Experimental Attention. Life 2015;5(1):294–320.
7. Carvalho ATP, Fernandes PA and Ramos MJ. The Catalytic Mechanism of RNA Polymerase II. J Chem Theory Comput 2011;7(4):1177–1188; doi: 10.1021/ct100579w.
8. Cech TR. It Was Long Thought That Every Cellular Reaction Is Catalyzed by a Protein Enzyme. The Discovery That RNA Can Cut, Splice and Assemble Itself Overturns the Principle-and Throws Light on Early Evolution. Sci Am 1986.
9. Chyba C and Sagan C. Endogenous Production, Exogenous Delivery and Impact-Shock Synthesis of Organic Molecules: An Inventory for the Origins of Life. Nature 1992;355(6356):125–132.
10. Cohen ZR, Todd ZR, Maibaum L, et al. Stabilization of Prebiotic Vesicles by Peptides Depends on Sequence and Chirality: A Mechanism for Selection of Protocell-Associated Peptides. Langmuir 2024;40(17):8971–8980; doi: 10.1021/acs.langmuir.4c00150.
11. Cohen ZR, Todd ZR, Wogan N, et al. Plausible Sources of Membrane-Forming Fatty Acids on the Early Earth: A Review of the Literature and an Estimation of Amounts. ACS Earth Space Chem 2022;7(1):11–27; doi: 10.1021/acsearthspacechem.2c00168.
12. Cornell CE, Black RA, Xue M, et al. Prebiotic Amino Acids Bind to and Stabilize Prebiotic Fatty Acid Membranes. Proc Natl Acad Sci 2019;116(35):17239–17244; doi: 10.1073/pnas.1900275116.
13. Dagar S, Sarkar S and Rajamani S. Nonenzymatic Template-Directed Replication Using 2'-3' Cyclic Nucleotides under Wet-Dry Cycles. 2022;2022.07.11.499554; doi: 10.1101/2022.07.11.499554.
14. Damer B and Deamer D. The Hot Spring Hypothesis for an Origin of Life. Astrobiology 2020;20(4):429–452; doi: 10.1089/ast.2019.2045.
15. Deamer BD and D. Coupled Phases and Combinatorial Selection in Fluctuating Hydrothermal Pools: A Scenario to Guide Experimental Approaches to the Origin of Cellular Life. Life 2015;872–887.
16. Deamer W. D. Boundary Structures Are Formed by Organic Components of the Murchison Carbonaceaous Chondrite. Nature 1985;317:792–794.

17. Duzdevich D, Carr CE, Ding D, et al. Competition between Bridged Dinucleotides and Activated Mononucleotides Determines the Error Frequency of Nonenzymatic RNA Primer Extension. Nucleic Acids Res 2021;49(7):3681–3691.
18. Gánti T. The Principles of Life. Oxford University Press; 2003.
19. Gilbert W. Origin of Life: The RNA World. Nature 1986;319(6055):618–618; doi: 10.1038/319618a0.
20. Good NE, Winget GD, Winter W, et al. Hydrogen Ion Buffers for Biological Research*. Biochemistry 1966;5(2):467–477; doi: 10.1021/bi00866a011.
21. Guttenberg N, Virgo N, Chandru K, et al. Bulk Measurements of Messy Chemistries Are Needed for a Theory of the Origins of Life. Philos Trans R Soc Math Phys Eng Sci 2017;375(2109); doi: 10.1098/rsta.2016.0347.
22. Hargreaves WR and Deamer DW. Liposomes from Ionic, Single-Chain Amphiphiles. Biochemistry 1978;17(18):3759–3768; doi: 10.1021/bi00611a014.
23. Hoffman MM, Khrapov MA, Cox JC, et al. AANT: The Amino Acid–Nucleotide Interaction Database. Nucleic Acids Res 2004;32(Database issue):D174–D181; doi: 10.1093/nar/gkh128.
24. Ikehara K. Possible Steps to the Emergence of Life: The [GADV]-Protein World Hypothesis. Chem Rec 2005;5(2):107–118; doi: 10.1002/tcr.20037.
25. Ikehara K. [GADV]-Protein World Hypothesis on the Origin of Life. Orig Life Evol Biosph 2014;44(4):299–302; doi: 10.1007/s11084-014-9383-4.
26. Ishigami T, Suga K and Umakoshi H. Chiral Recognition of L-Amino Acids on Liposomes Prepared with l-Phospholipid. ACS Appl Mater Interfaces 2015;7(38):21065–21072; doi: 10.1021/acsami.5b07198.
27. Jeong E, Kim H, Lee S-W, et al. Discovering the Interaction Propensities of Amino Acids and Nucleotides from Protein-RNA Complexes. Mol Cells 2003;16(2):161–167; doi: 10.1016/S1016-8478(23)13783-6.
28. Joshi MP, Steller L, Van Kranendonk MJ, et al. Influence of Metal Ions on Model Protoamphiphilic Vesicular Systems: Insights from Laboratory and Analogue Studies. Life 2021;11(12):1413; doi: 10.3390/life11121413.
29. Joshi MP, Uday A and Rajamani S. Elucidating N-Acyl Amino Acids as a Model Protoamphiphilic System. Commun Chem 2022;5(1):147.
30. Koga T and Naraoka H. A New Family of Extraterrestrial Amino Acids in the Murchison Meteorite. Sci Rep 2017;7(1):636; doi: 10.1038/s41598-017-00693-9.
31. Lawless JG and Yuen GU. Quantification of Monocarboxylic Acids in the Murchison Carbonaceous Meteorite. Nature 1979;282(5737):396–398.
32. Mansy SS. Membrane Transport in Primitive Cells. Cold Spring Harb Perspect Biol 2010;2(8):a002188–a002188; doi: 10.1101/cshperspect.a002188.
33. Mansy SS and Szostak JW. Reconstructing the Emergence of Cellular Life through the Synthesis of Model Protocells. Cold Spring Harb Symp Quant Biol 2009;74:47–54; doi: 10.1101/sqb.2009.74.014.

34. Maurer S. The Impact of Salts on Single Chain Amphiphile Membranes and Implications for the Location of the Origin of Life. Life 2017;7(4):44; doi: 10.3390/life7040044.
35. Mayer C, Schreiber U, Dávila MJ, et al. Molecular Evolution in a Peptide-Vesicle System. Life 2018;8(2):16; doi: 10.3390/life8020016.
36. McCollom TM, Ritter G and Simoneit BRT. Lipid Synthesis Under Hydrothermal Conditions by Fischer- Tropsch-Type Reactions. Orig Life Evol Biosph 1999;29(2):153–166; doi: 10.1023/A:1006592502746.
37. Miller SL. A Production of Amino Acids Under Possible Primitive Earth Conditions. Science 1953;117(3046):528–529; doi: 10.1126/science.117.3046.528.
38. Miller SL and Cleaves HJ. Prebiotic Chemistry on the Primitive Earth. Syst Biol 2006;1:1.
39. Mishra S and Chakraborty H. Phosphatidylethanolamine and Cholesterol Promote Hemifusion Formation: A Tug of War between Membrane Interfacial Order and Intrinsic Negative Curvature of Lipids. J Phys Chem B 2023;127(36):7721–7729; doi: 10.1021/acs.jpcb.3c04489.
40. Monnard P-A. Taming Prebiotic Chemistry: The Role of Heterogeneous and Interfacial Catalysis in the Emergence of a Prebiotic Catalytic/Information Polymer System. Life 2016;6(4):40.
41. Monnard P-A and Deamer DW. Preparation of Vesicles from Nonphospholipid Amphiphiles. Methods Enzymol 2003;372:133–151; doi: 10.1016/S0076-6879(03)72008-4.
42. Namani T and Walde P. From Decanoate Micelles to Decanoic Acid/Dodecylbenzenesulfonate Vesicles. Langmuir ACS J Surf Colloids 2005;21(14):6210–6219; doi: 10.1021/la047028z.
43. Orgel LE. Prebiotic Chemistry and the Origin of the RNA World. Crit Rev Biochem Mol Biol 2004;39(2):99–123; doi: 10.1080/10409230490460765.
44. Patel BH, Percivalle C, Ritson DJ, et al. Common Origins of RNA, Protein and Lipid Precursors in a Cyanosulfidic Protometabolism. Nat Chem 2015;7(4):301–307; doi: 10.1038/nchem.2202.
45. Patki GM and Rajamani S. Nonenzymatic RNA Replication in a Mixture of “spent” Nucleotides. FEBS Lett 2023; doi: 10.1002/1873-3468.14785.
46. Pielak GJ. Buffers, Especially the Good Kind. Biochemistry 2021;60(46):3436–3440; doi: 10.1021/acs.biochem.1c00200.
47. Rajamani S, Ichida JK, Antal T, et al. Effect of Stalling after Mismatches on the Error Catastrophe in Nonenzymatic Nucleic Acid Replication. J Am Chem Soc 2010;132(16):5880–5885; doi: 10.1021/ja100780p.
48. Romero Nieto D, Lindbråthen A and Hägg M-B. Effect of Water Interactions on Polyvinylamine at Different pHs for Membrane Gas Separation. ACS Omega 2017;2(11):8388–8400; doi: 10.1021/acsomega.7b01307.
49. Rout SK, Wunnava S, Krepl M, et al. Amino Acids Catalyse RNA Formation under Ambient Alkaline Conditions. Nat Commun 2025;16(1):5193; doi: 10.1038/s41467-025-60359-3.
50. Roy R, Sawant AA and Rajamani S. Cross-Catalytic Enhancement of Peptides and RNA from a Common Prebiotic Activated Intermediate. 2024;2024.10.02.616211; doi:

10.1101/2024.10.02.616211.

51. Sanchez C and Renard D. Stability and Structure of Protein-Polysaccharide Coacervates in the Presence of Protein Aggregates. Int J Pharm 2002;242(1–2):319–324; doi: 10.1016/S0378-5173(02)00174-6.
52. Sarkar S, Dagar S and Rajamani S. Front Cover: Influence of Wet–Dry Cycling on the Self-Assembly and Physicochemical Properties of Model Protocellular Membrane Systems (ChemSystemsChem 5/2021). ChemSystemsChem 2021;3(5); doi: 10.1002/syst.202100033.
53. Sarkar S, Das S, Dagar S, et al. Prebiological Membranes and Their Role in the Emergence of Early Cellular Life. J Membr Biol 2020;(0123456789); doi: 10.1007/s00232-020-00155-w.
54. Simoneit BR, Rushdi AI and Deamer DW. Abiotic Formation of Acylglycerols under Simulated Hydrothermal Conditions and Self-Assembly Properties of Such Lipid Products. Adv Space Res 2007;40(11):1649–1656.
55. Suga K, Tauchi A, Ishigami T, et al. Preferential Adsorption of L-Histidine onto DOPC/Sphingomyelin/3β-[N-(N',N'-Dimethylaminoethane)Carbamoyl]Cholesterol Liposomes in the Presence of Chiral Organic Acids. Langmuir 2017;33(15):3831–3838; doi: 10.1021/acs.langmuir.6b03264.
56. Szostak JW. The Eightfold Path to Non-Enzymatic RNA Replication. J Syst Chem 2012;3(1):2; doi: 10.1186/1759-2208-3-2.
57. Tauchi A, Suga K and Umakoshi H. Hydrolase-Like Activity Provided by Zinc(II) and Oleoyl-Histidine at Liposome Membrane Surface. Colloids Interfaces 2018;2(2):24; doi: 10.3390/colloids2020024.
58. Vincent L, Colón-Santos S, Cleaves HJ, et al. The Prebiotic Kitchen: A Guide to Composing Prebiotic Soup Recipes to Test Origins of Life Hypotheses. Life 2021;11(11):1221.
59. Vogel SR, Deck C and Richert C. Accelerating Chemical Replication Steps of RNA Involving Activated Ribonucleotides and Downstream-Binding Elements. Chem Commun 2005;(39):4922–4924; doi: 10.1039/B510775J.
60. Walton T, Zhang W, Li L, et al. The Mechanism of Nonenzymatic Template Copying with Imidazole-Activated Nucleotides. Angew Chem Int Ed 2019;58(32):10812–10819; doi: 10.1002/anie.201902050.
61. Xue M, Black RA, Cohen ZR, et al. Binding of Dipeptides to Fatty Acid Membranes Explains Their Colocalization in Protocells but Does Not Select for Them Relative to Unjoined Amino Acids. J Phys Chem B 2021;125(29):7933–7939; doi: 10.1021/acs.jpcb.1c01485.

Figures

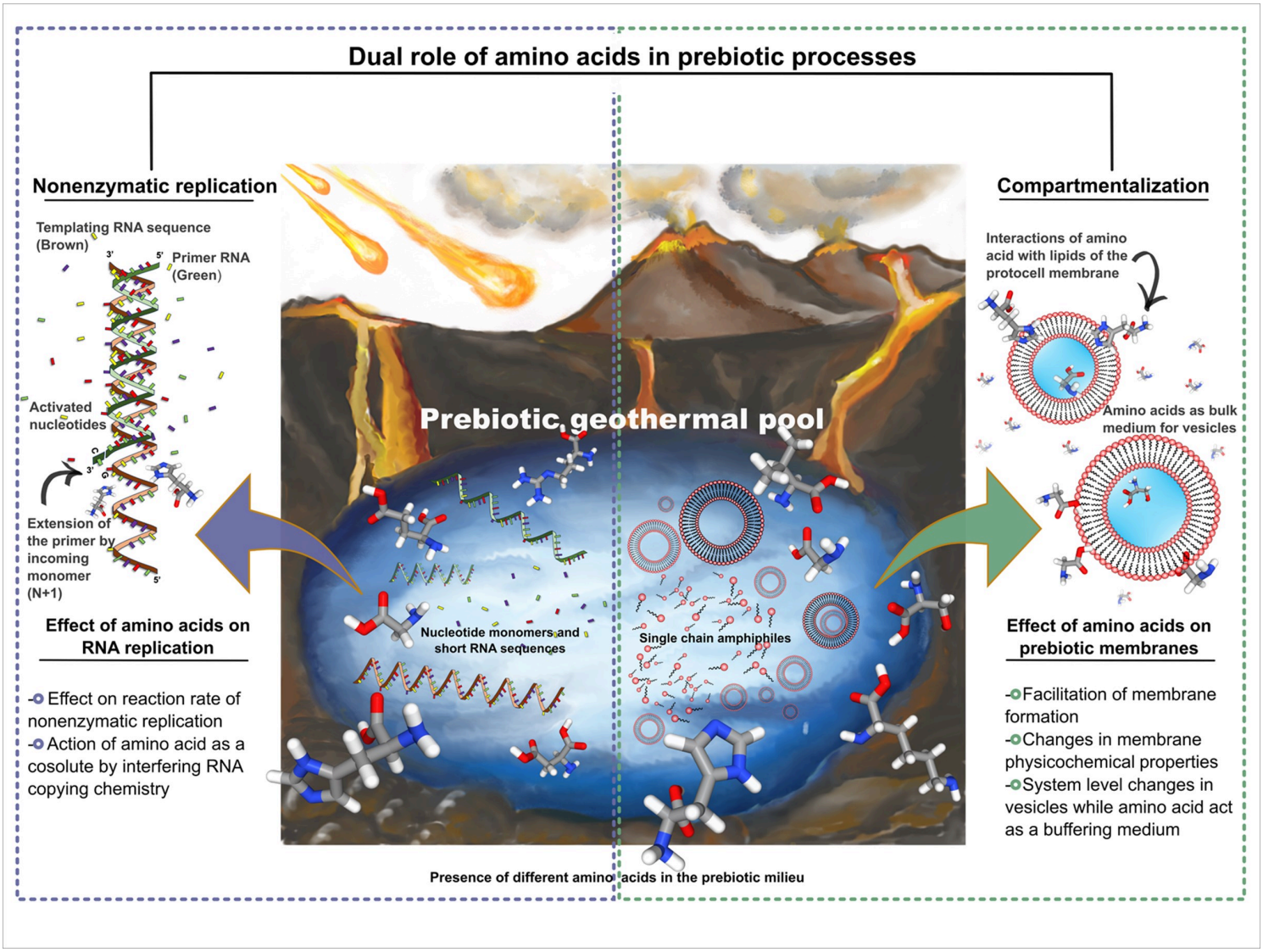

Figure 1

The schematic depiction of the dual role of amino acid monomers in nonenzymatic RNA replication (left panel, blue dotted box) and prebiotic compartmentalization (right panel, green dotted box). The background is of a hypothetical early Earth geothermal pool niche, which depicts molecules in a heterogeneous prebiotic milieu. In the case of nonenzymatic replication (left panel), the coexistence of amino acid monomers (stick models) along with the template sequence and the primer RNA (the brown and green colour strands, respectively, in the RNA cartoon), impacts the incoming monomers' addition during the copying of information (activated nucleotides, multicoloured floating molecules). In case of prebiotic compartmentalization (right panel), these amino acid monomers act as a buffering agent while coexisting with fatty acids, and facilitate robust vesicle formation even at suboptimal pH.

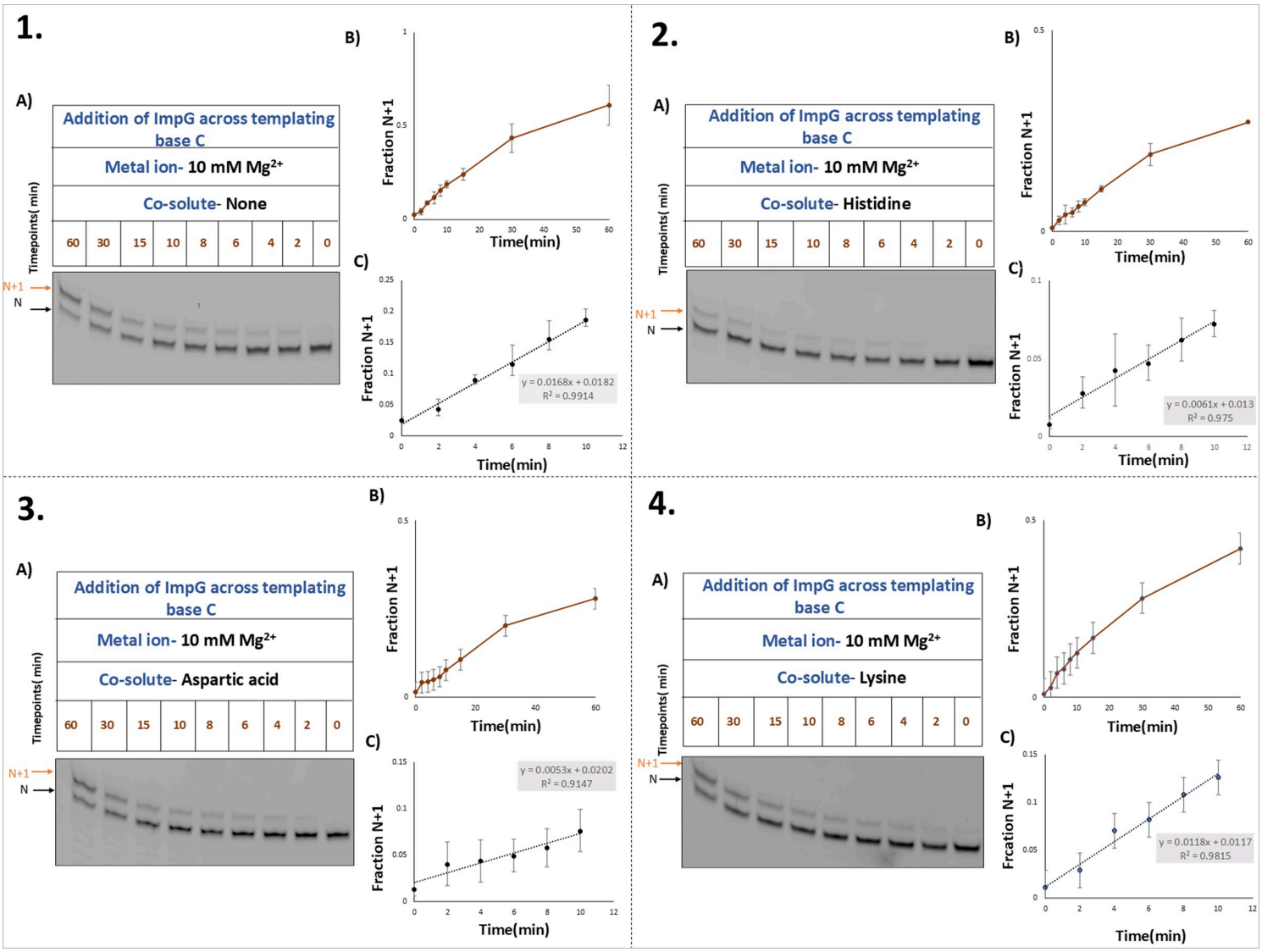

Figure 2

The effect of amino acids on the rate of ImpG addition against templating base C. Panel 1 represents the control G_C reactions. Panel 2 represents neutral charged candidate (Histidine) reactions. Panel 3 and 4 represents negatively charged candidate (Aspartic acid) and positively charged amino acid candidate (Lysine) reactions respectively. Subpanels A represent 20% urea gels for a single reaction from each reaction sets (images are contrast adjusted by using ImageJ software) whereas subpanels B represent the whole fit representing the reaction kinetics for each reaction set. Subpanels C show how the initial rates of the reactions are obtained by fitting the early data points in the linear regime. The rates are calculated by multiplying the slope of the linear curve with 60, which gives the rate/hour ($hour^{-1}$). The error bars represent the standard deviation (N=3) for each reaction set.

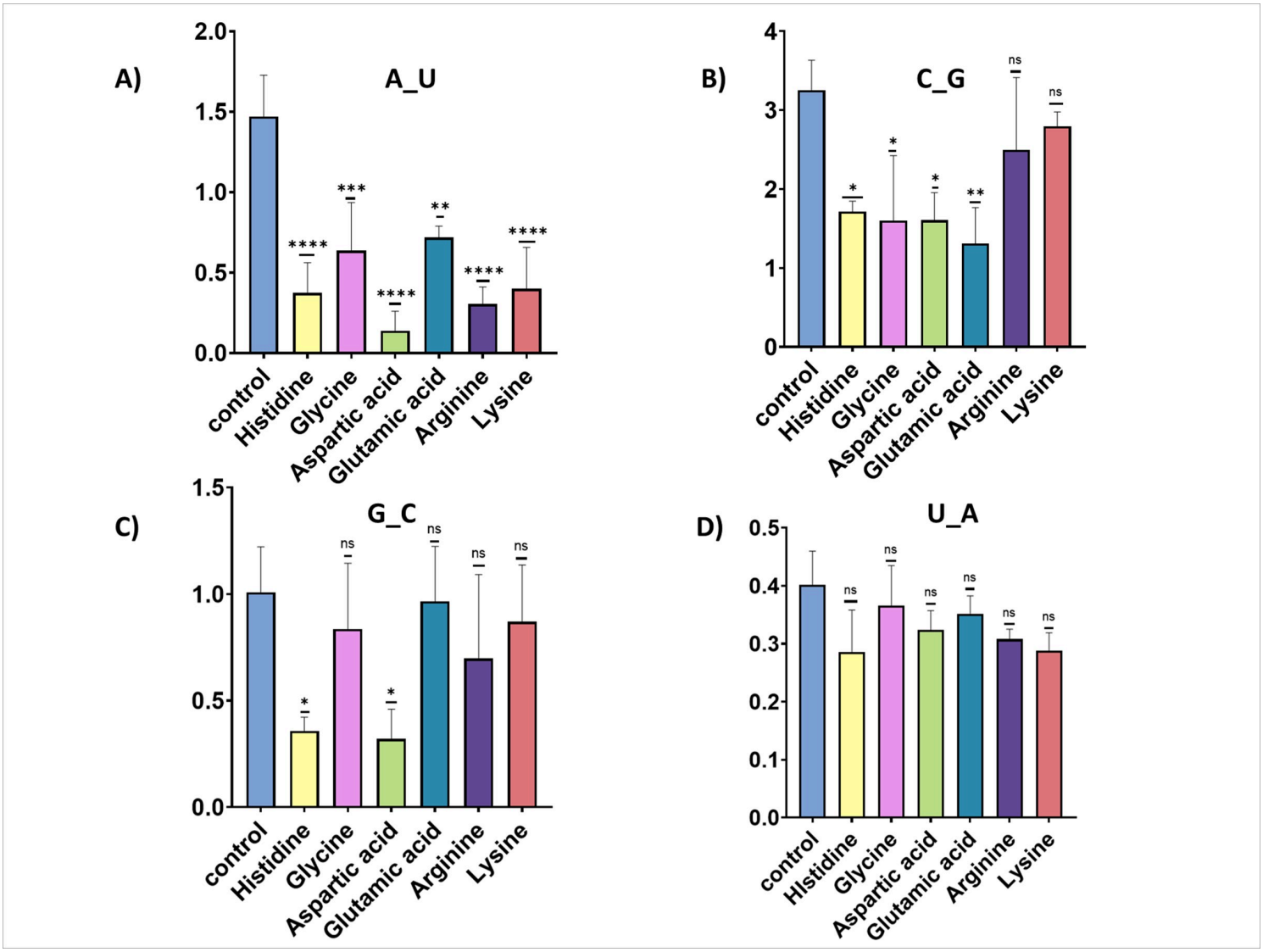

Figure 3

Effect of six different amino acids on the rate of nonenzymatic template-directed reactions. Panels indicate: A) A_U reaction; B) C_G reaction; C) G_C reaction; D) U_A reactions, respectively. The error bars represent the standard deviation. The statistical analysis was done using GraphPad Prism 10.4.1 software; a One-Way ANOVA test was performed by comparing the mean of the control reaction with the mean of each reaction carried out in the presence of the amino acids; $P< 0.05$, [N=3].

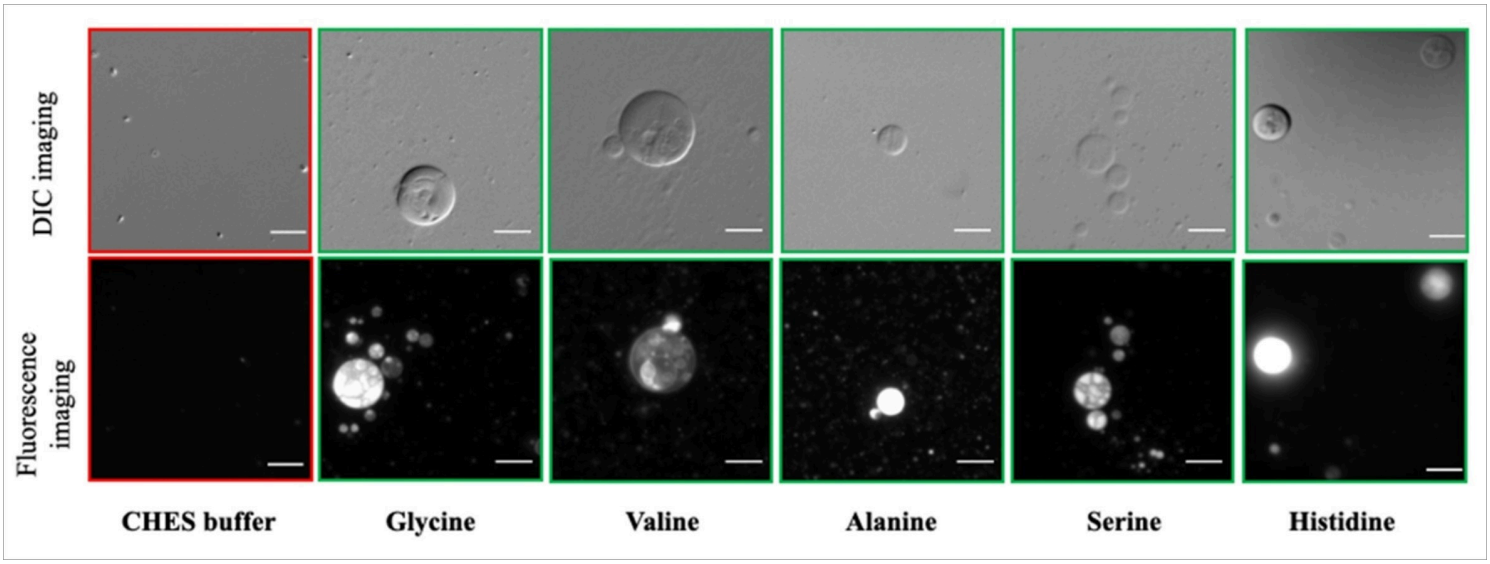

Figure 4

Differential interference contrast (DIC, top panel) and fluorescence microscopy images (bottom panel) of oleic acid vesicles in different amino acid buffers of glycine, valine, alanine, serine and histidine at 200 mM concentration, pH ~ 9.6 (green boxes). Corresponding control is shown with pH ~9.6 CHES buffer (red box) where no oleic acid vesicle is observed. Scale bars are 10 μm.

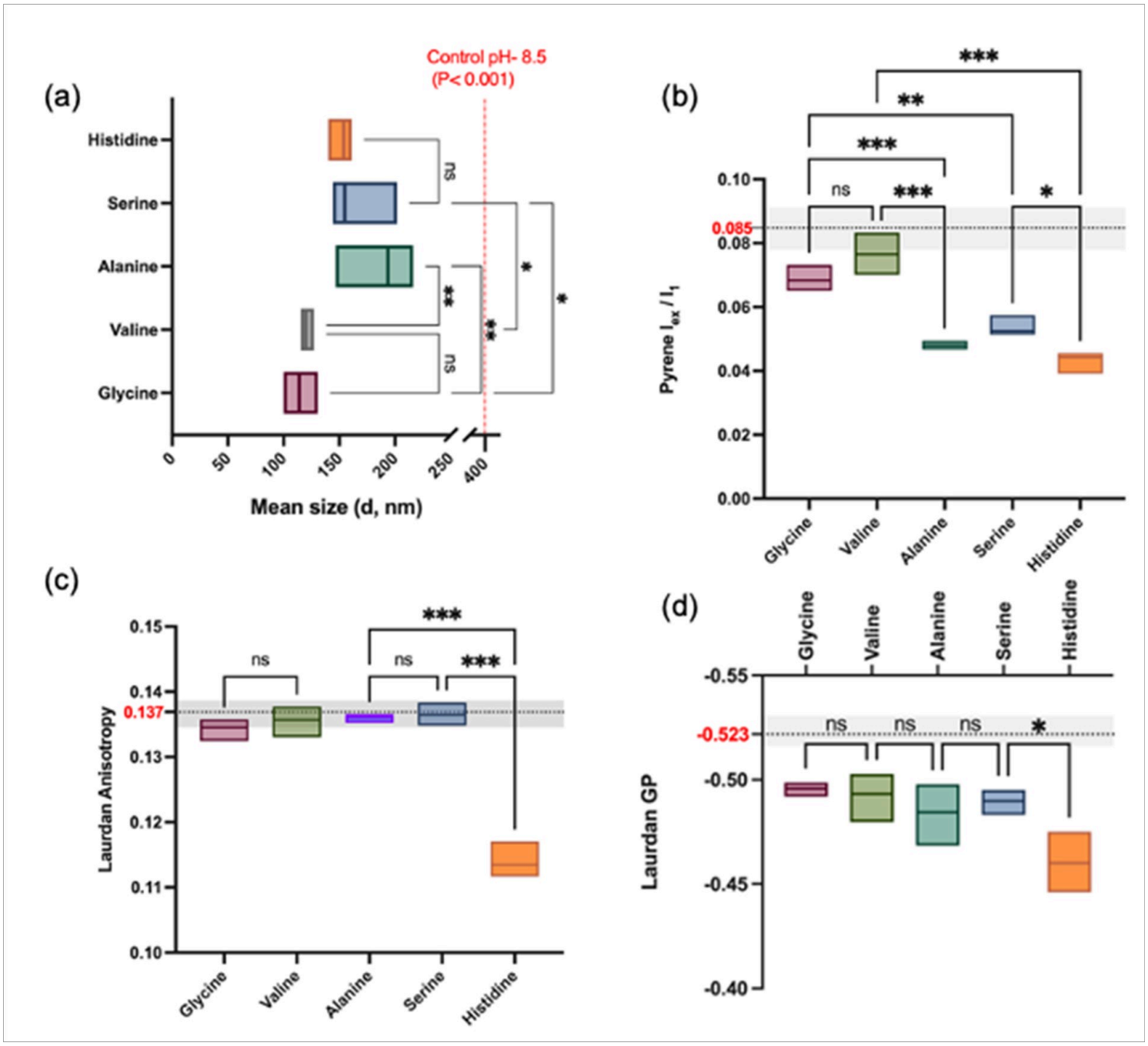

Figure 5

(a) Mean hydrodynamic radii of vesicles (size, in nm) obtained for the vesicles formed in different amino acid solutions. All of the amino acid buffers had vesicles of lower mean size than what was seen in the optimum control condition for oleic acid vesicles at pH- 8.5 (marked by red dashed line). (b) Pyrene I_{ex}/I_1 ratio depicting the total bilayer content in corresponding amino acid solutions. (c) The Laurdan anisotropy obtained value for vesicles present in different amino acid solutions. (d) Laurdan GP value plot for vesicles formed in different amino acid solutions. In panels b-d, the black dashed line indicates the corresponding value for control vesicles obtained at the optimum condition of pH-8.5 in a relevant Goods buffer. All the plots are box plots with the centre line showing the mean value, and upper and

lower edges of the box depicting the upper and lower ranges of the corresponding values. For the control dashed line, grey shade indicates the range of the values obtained.

Supplementary Files

This is a list of supplementary files associated with this preprint. Click to download.

- SIAstrobiologyAST.docx